Self-Supervised Antipodal Grasp Learning with Fine-Grained Grasp Quality Feedback in Clutter

Yanxu Hou, Jun Li, *Senior Member, IEEE*, and I-Ming Chen, *Fellow, IEEE*

***Abstract*—It is a challenging goal in robotics to make a robot grasp like a human being in a cluttered environment. Self-supervised grasp learning is one of the most promising approaches to human-like robotic grasp. However, due to inadequate feedback on grasp quality, almost the existing self-supervised grasp learning methods are coarse-grained. This paper proposes a fine-grained antipodal grasp learning (FAGL) method with augmented learning feedback. First, an indicator called antipodal degree of a grasp (ADG) is defined by a non-increasing monotonous function to reflect fine-grained grasp quality. It can be evaluated indirectly by the destructive effect of a grasp on the environment via scene images. Next, we design a restorative sampling strategy to collect the samples of fine-grained antipodal grasps and propose a refined affordance network to generate grasp affordance maps for FAGL to decide grasp policies. Finally, in grasping actual metal workpieces, FAGL outperforms its peers in terms of grasp success rate and ADG in cluttered scenarios by reducing the grasp effects on the surroundings. Extensive experiments show that our method has great potential for industrial application.**

***Index Terms*—Robotic grasp, antipodal degree, cluttered objects, deep reinforcement learning, affordance map.**

I. INTRODUCTION

HUMAN-LIKE grasp is one of the challenging long-term goals in robotics [1]–[5]. In recent years, robots can learn to grasp by trial and error via advanced learning-based approaches [6]–[10]. Unfortunately, it is far from a human-like grasp in terms of flexibility, adaptability, and reliability. Humans can successfully grasp various objects, even the unseen, in different environments. Moreover, a grasp by a human being inclines to be antipodal. Namely, it is a reliable grasp without perturbations to its environment. In robotics, an antipodal grasp is usually characterized by force closure (FC) [11] and no collision with surroundings [12]. Specifically, force closure can be reflected by the connecting line of the two contact points parallel to the movement direction of the fingers [17], or the connecting line of the two contact points is located in their friction cone [23]. Self-supervised grasp learning (SGL) is one of the most promising approaches to human-like antipodal grasp [7], [8], [10]. Nevertheless, insufficient feedback or rewards of SGL is a crucial obstacle to pursuing antipodal grasps for a robot. Motivated by it, we augment the feedback of SGL by estimating the destructive effect of a grasp on the environment and propose a new SGL method for learning fine-grained antipodal grasp in clutter.

Traditional analytical grasp methods, such as in [4], [11]–[14], can only decide whether or not a grasp is antipodal but cannot identify how antipodal a grasp is. In addition, analytical grasp methods extremely rely on accurate physical models of end-effectors and objects to be grasped and hold a strict assumption on friction coefficients. Therefore, they do not apply to unseen objects and complex scenarios with many kinds of objects in clutter, as a human being does.

Recently, the emerging learning-based grasp methods [3], [6]–[8], [15], enjoy high generalizability to grasp unseen objects in cluttered environments. They learn a grasp through training and observing visual scenes, not requiring the physical models of end-effectors and objects. Self-supervised grasp learning [3], [7], [8], [10], [16] as a typical learning-based grasp method can learn an optimal grasp policy by trials and errors. It does not require accurate estimation of the poses of an object and manual sample annotations. However, a grasp is likely not antipodal due to undesired movements of the objects to be grasped or incurred destructive effects on the surroundings. Generally, such a grasp is of low quality even though it is successful. The inadequate feedback for grasp learning leads to low-quality grasps. The feedback of the existing approaches in [7], [8], [10], [16] reflects only the success or failure of a grasp instead of antipodal degrees. As a result, they may fail to achieve a fine-grained antipodal grasp. On the other hand, the previous related works show that augmented feedback can significantly improve the performance of self-supervised learning in various applications, e.g., video games in [17], continuous robot control in [18], and intelligent transport systems in [19]. However, to the authors' best knowledge the feedback of grasp learning has been augmented seldom in literature. The reason is likely that it is difficult to make a fine-grained evaluation on grasp quality in image space without the physical models of objects and grippers for SGL.

This paper proposes an indicator of the destructive effect of a grasp (DEG) on the environment to evaluate the grasp quality. It

This work was supported in part by the National key research and development program of China under Grant 2021YFF0500904, and Shenzhen Fundamental Research Program under Grant JCYJ20190813152401690. (Corresponding author: Jun Li.)

Y. Hou and J. Li are with the Ministry of Education Key Laboratory of Measurement and Control of CSE, Southeast University, Nanjing 210096, China (e-mail: yxhou@seu.edu.cn; j.li@seu.edu.cn).

I.-M. Chen is with the School of Mechanical and Aerospace Engineering, Nanyang Technological University, Singapore 639798 (e-mail: MIChen@ntu.edu.sg).

quantifies the difference between the images of scenes before grasping an object and after putting it back to the home position. Note that putting back an object is only set for grasp training but not happening in a real grasp. Moreover, an antipodal degree of grasp (ADG) is transformed from DEG for evaluating the action quality of grasp and is leveraged to augment the feedback of grasp learning.

The main contributions of this work are as follows.

1) We propose for the first time DEG to reflect a grasp effect on the environment and then define ADG by DEG to evaluate the grasp quality in a fine-grained manner. ADG can be assessed in image space requiring no models of grippers and objects. ADG is fine-grained in total contrast to either coarse-grained or even binary grasp quality assessed by antipodal constraints in point clouds. In a word, ADG provides a novel and fine way to evaluate grasp quality in the image space, compared with traditional analytic methods.
2) We propose a fine-grained antipodal grasp learning (FAGL) whose feedback is augmented by ADG. A restorative sampling strategy (RSS) is designed to collect the samples of fine-grained antipodal grasps. RSS ensures the consistency of the trajectories of picking an object up and placing it back to reduce the negative effects on the surroundings. Additionally, a Refined Affordance Network (RA-Net) is presented to output grasp affordances to infer fined-grained antipodal grasps. FAGL is expected to realize human-like grasp in various environments, especially suitable for applications with a low tolerance for perturbations.
3) Extensive grasp experiments are conducted on actual metal workpieces in clutter for the first time. The results demonstrate that FAGL is superior to its peers in reducing environment perturbations without losing grasp success rate.

The remainder of this paper is organized as follows. Section II recalls the related work. DEG and ADG are formulated in Section III, and FAGL is presented in Section IV. Extensive experiments are conducted in Section V. Section VI concludes the work.

II. Related Work

A. Self-Supervised Grasp Learning

By self-supervised grasp learning, a robot can learn an optimal grasp policy by trial-and-error in the environment, requiring no physical models of objects and massive annotated samples. Such methods have been paid extensive attention over the past few years. Pinto *et al*. [3] first tried self-supervised grasp learning and reached a grasp success rate of 95% in the cluttered scenes. Levine *et al*. [10] utilized multiple robots to collect samples in parallel for several months to improve the performances of self-supervised grasp learning. Zeng *et al*. [7] combined pushing with grasping into their Deep Q Network (DQN), thereby gaining a high grasp success rate and efficiency in grasping closely arranged-objects. Kalashnikov *et al*. [16] realized closed-loop grasping via DRL. To improve the learning efficiency of DRL, Liu *et al*. [20] proposed an active exploration strategy in grasping.

Although the prior methods focus on achieving a high grasp success rate, it may lead to a grasp of low quality, e.g., a unrobust grasp apt to perturb environments. On the other hand, several enlightening studies have indicated that image differences can represent the quality of robot manipulation. For example, Berscheid *et al*. [21] implemented goal-conditional placement with high precision by using a contrastive loss and the image difference between the scenes before pickup and after placing as a placing reward. Other studies find that robots can learn to grasp in an antipodal way by learning antipodal grasp samples. As known, the more antipodal a grasp, the more reliable the grasp is. Cai *et al*. [8] proposed a corrective grasp strategy to collect antipodal grasp samples. It is a pioneer in learning antipodal grasp in a self-supervised learning manner. Unfortunately, this method does not take grasp quality into account and can only apply to antipodal grasp of single objects. The above two methods exclude grasping in a cluttered environment.

The methods mentioned above cannot afford high-quality grasps due to inadequate feedback for grasp learning. As known, augmenting feedback or rewards of DRL is one of the most common technologies for improving learning performances of DRL.

B. Grasp Quality Evaluation

Grasp quality indicates the performances of a grasp, e.g., robustness, stability, and reliability [12], [13], [22], [23]. Generally, grasp quality is evaluated by analytical methods such as FC criterion and Grasp Wrench Space (GWS) analysis [4], [12]. The analytical techniques require manual features of sensing data to score overall grasp quality. On the other hand, more recent methods evaluate grasp quality by justifying antipodal conditions given in [12]. The antipodal conditions are that (1) the connecting line of the grasp points lies inside the friction cone of the grasp points, and (2) the end-effector does not collide with the environment. For example, Mahler *et al*. [24] determined the grasp quality by using robust quasi-static GWS analysis. Based on the work in Mahler *et al*. [24], Satish *et al*. [25] proposed fully convolutional grasp quality CNN (FC-GQ-CNN) to predict high quality grasps. Qin *et al*. [26] evaluated a grasp quality with an antipodal score according to the angle between the connecting line of the two grasp contact points and the face normal of the object at contact points. Liang *et al*. [27] designed a multi-level grasp quality metric, considering that the smaller the coefficient of friction required for successful grasps, the higher the antipodal score. Unfortunately, the grasp quality defined by the methods mentioned above is coarse or even binary. In addition, the antipodal conditions are insufficient to cover all the situations of perturbations to the environment. In the scenarios with separate objects, an antipodal grasp can successfully avoid perturbations to the surroundings of objects [8], [24]. However, it may fail to grasp occluded objects. Furthermore, to evaluate grasp quality by the antipodal conditions necessitates physical models or accurate point clouds of

a parallel gripper and objects to be grasped. Nevertheless, actual point clouds inevitably contain noise. It may lead to an inaccurate estimation of grasp quality by misidentifying the coordinates and face normals of objects using noisy point clouds within the Darboux frame [27].

Although some methods, e.g., [13], [22], [23], attempted to identify directly grasp quality in image space, it is possible for them to misidentify grasp quality, particularly in cluttered environments. Because they rely on manual visual features highly relying on accurate edge detection. Other methods also claim that they can predict grasp quality from raw images [26]–[28]. But, they need a labeled dataset in which the grasp quality is calculated using analytic methods.

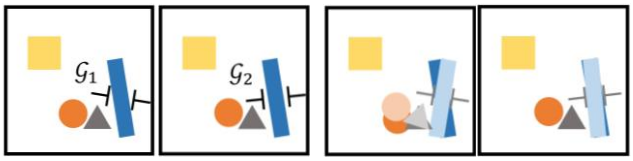

Fig. 1. Grasp effects on the environment. (a) and (b) show two different grasps $\mathcal{G}_1$ and $\mathcal{G}_2$ to be performed in the same environment. Both (c) and (d) show a scenario after grasping a rectangle block, where the light and dark rectangles indicate the position of the block before and after grasping, respectively.

III. ADG FOR GRASP QUALITY EVALUATION

Traditional analytic methods cannot provide a comprehensive and fine-grained grasp quality metric for self-supervised grasp learning. This paper defines ADG as an indirect evaluation of grasp quality in a thorough and fine-grained manner by transforming DEG into a non-increasing monotonic function.

A. Destructive Effect of Grasp

Definition 1: A restorative manipulation $\mathcal{M} = (\mathcal{T}, \mathcal{T}^-)$, represents the process that a robot picks up an object along a trajectory $\mathcal{T}$ and then places back it along the inverse trajectory $\mathcal{T}^-$.

Definition 2: Destructive effect of a grasp (DEG) $\mathcal{P}$ reflects the destruction caused by grasp $\mathcal{G}$ on the environment by,

$$\mathcal{P} = \frac{\|\mathcal{B}(I_{hc}^-) - \mathcal{B}(I_{hc}^+)\|^1}{H \times W}, \tag{1}$$

where I_{hc}^- and I_{hc}^+ represent the color heightmap of the environment before and after performing restorative manipulation M, respectively. $\mathcal{B}$ denotes an OTSU operation that converts an image to a binary image. H and W are the same weight and height of I_{hc}^- and I_{hc}^+ , respectively.

$\mathcal{P} \neq 0$ refers to the change in scenes before grasping the object and after putting it back. It considers only scene changes caused by the restorative manipulation of an object but not the scene difference between before and after the grasp. The restorative manipulation ensures that the equivalence of different grasp tries. Moreover, Eq. (1) excludes the influence of the size of images by dividing $H \times W$. It leads to $\mathcal{P} \in [0,1]$.

$\mathcal{P} = 0$ means that $\mathcal{G}$ does not destroy the environment. The larger $\mathcal{P}$ is, the greater the impact on the environment is. Therefore, DEG, i.e., $\mathcal{P}$ intuitively reflects destructions of $\mathcal{G}$ on the environment in image space. Next, we define an antipodal degree of a grasp (ADG) by DEG.

B. Antipodal Degree of Grasp

Definition 3: An antipodal degree of a grasp (ADG) $\mathcal{A}$ is a function for evaluating the action quality of a grasp by DEG,

$$\mathcal{A} = -\mathcal{P} + 1, \mathcal{P} \in [0,1] \subset \mathbb{R}. \tag{2}$$

$\mathcal{A}$ can be any non-increasing monotonic function. The better ADG is, the smaller DEG is, and vice versa. ADG can assess grasp quality in a fine-grained manner since it is transformed from a continuous $\mathcal{P}$ via a continuous non-increasing monotonic function. It suggests that grasp quality can be indirectly obtained in image space using ADG, requiring no analysis of the point cloud of objects.

For example, figure 1 illustrates the effect of different grasps on the environment. Specifically, although both $\mathcal{G}_1$ and $\mathcal{G}_2$ successfully grasp the blue block, $\mathcal{G}_1$ results in a larger change than $\mathcal{G}_2$. It indicates that DEG of $\mathcal{G}_1$ is greater than that of $\mathcal{G}_2$, namely, ADG of $\mathcal{G}_1$ is inferior to that of $\mathcal{G}_2$.

Compared with the binary grasp quality metric in [28] and point cloud-based analysis in [12], ADG is more comprehensive since DEG can reflect all the destructions in a grasp environment. Apparently, ADG applies to the grasping of cluttered objects. For instance, even if a grasp satisfies antipodal constraints, it may lead to unexpected movements of the surrounding objects in cluttered scenes. In such a case, ADG is still effective, while the analysis-based grasp quality metrics in [20] [32] are not. In a word, ADG is a substantial progress in grasp quality evaluation.

IV. Fine-grained Antipodal Grasp Learning

A. Problem Formulation

A fixed mounted RGB-D camera is used to capture color and depth images, and a 6-DoF manipulator equipped with a parallel gripper is harnessed to grasp an object. A grasp $\mathcal{G}$ is formulated as a tri-tuple,

$$\mathcal{G} = (T, \phi, \omega), \tag{3}$$

where $T = (x, y, z)$, ϕ, and ω denote the position, rotation around Z-axis, and initial distance between the two fingers of the gripper, respectively. An RGB-D image $I = (I_c, I_d)$, including an RGB image I_c and a depth map I_d .

Self-supervised grasp learning can be formulated as a five-tuple Markov Decision Process (MDP) $\langle \mathcal{O}, \mathcal{G}, \mathcal{R}, \rho, \mathcal{H} \rangle$, where $\mathcal{O}$, $\mathcal{G}$, $\mathcal{R}$, ρ, and $\mathcal{H}$ denote the observation space, robotic grasp space, feedback (rewards), a transition probability, and the maximum step till termination, respectively. Given $\mathcal{O}_t$ at time t, a robot executes grasp $\mathcal{G}_t$ following a grasp policy, resulting in environment feedback $\mathcal{R}_t$. Then, $\mathcal{O}_t$ transits to $\mathcal{O}_{t+1}$ following ρ. We set $\mathcal{H} = 1$ to treat the self-supervised grasp learning as one-step reinforcement learning as Levine *et al.* [10] do. The learning goal is to find an optimal grasp policy to maximize the expected feedback through learning in a replay buffer $D = \{(\mathcal{O}_i, \mathcal{G}_i, \mathcal{R}_i)\}_{i \in [1,N]}$, where N is the size of D.

B. Double DQN-Based Grasp Learning

Figure 2 shows the architecture of FAGL and the learning process of an optimal grasp policy.

Unlike DQN-based grasp learning [7], FAGL leverages a double DQN [29] to learn an optimal grasp policy that is determined by an action-value function $Q_\theta(\mathcal{O}, \mathcal{G})$,

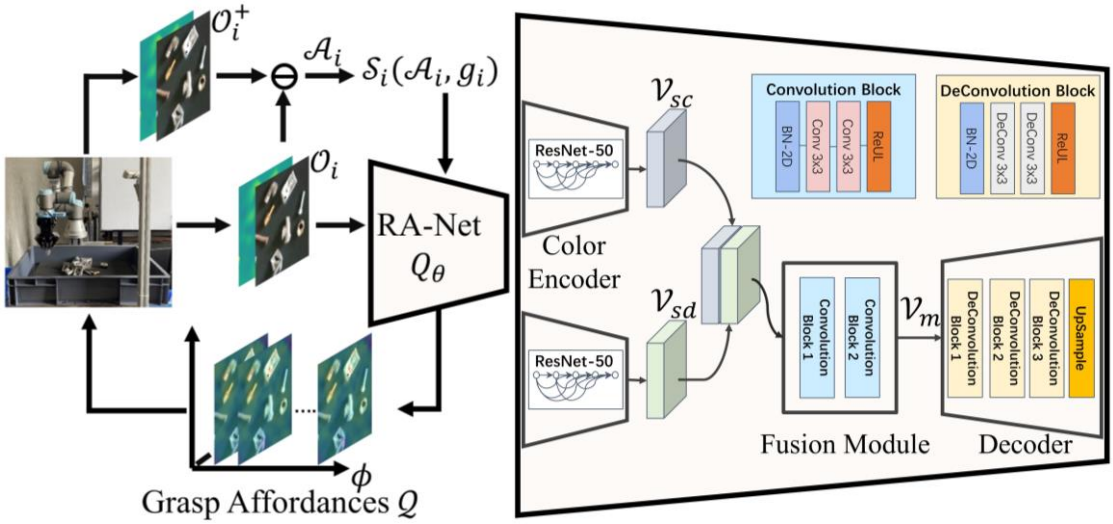

Fig. 2. The architecture of fine-grained antipodal grasp learning (FAGL). (a) The process of FAGL and (b) RA-Net.

$$\mathcal{G} = \underset{\mathcal{G}}{argmax} Q_\theta(\mathcal{O}, \mathcal{G}). \tag{4}$$

Double DQN reduce overestimations in DQN [30] by decomposing the max operation in a target network into action selection and action evaluation. Double DQN-based grasp learning, such as [31], [32], has a positive effect on grasping accuracy and learning efficiency in comparison to DQN-based grasp learning methods.

An Refine Affordance Network (RA-Net) is designed to parameterize action-value function $Q_\theta(\mathcal{O}, \mathcal{G})$ to output multi-channel grasp affordance maps, where θ is the weights of network Q_θ. First, a camera captures current observation $\mathcal{O}_i$ and RA-Net accepts $\mathcal{O}_i$ as inputs and outputs grasp affordances with $\mathcal{G}$. Then, a robot attempts a grasp $\mathcal{G}$ of an object. Next, the camera captures $\mathcal{O}_i^+$ following RSS, and $\mathcal{A}_i$ and $\mathcal{R}_i(\mathcal{A}_i, g_i)$ is calculated. Finally, save $(\mathcal{O}_i, \mathcal{G}_i, \mathcal{R}_i)$ into D and update RA-Net. At each update iteration, we sample a batch of $\{(\mathcal{O}_i, \mathcal{G}_i, \mathcal{R}_i)\}_{i \in [0,B]}$ with batch size B from D and update θ by,

$$\theta \leftarrow \theta + \alpha \Delta_\theta \mathcal{L}(Q_\theta(\mathcal{O}, \mathcal{G}), y), \tag{5}$$

where $\mathcal{L}(Q_\theta(\mathcal{O}, \mathcal{G}), y)$ is the loss function of RA-Net and $y = \{y_i\}_{i \in [0,B]}$,

$$y_i = \mathcal{R}_i + \gamma Q_{\theta^-}\left(\mathcal{O}_i, \underset{\mathcal{G}}{argmax} Q_\theta(\mathcal{O}_i', \mathcal{G})\right), \tag{6}$$

where $\gamma = 1$ is a future feedback discount, $\mathcal{O}_i'$ is the next observation of $\mathcal{O}_i$, and Q_{θ^-} is a target RA-Net with parameters θ^- . After τ update, θ replaces θ^- to update target RA-Net. A mean squared error is used as $\mathcal{L}$ to train RA-Net.

$$\mathcal{L}(Q_\theta(\mathcal{O},\mathcal{G}),y)=\frac{1}{B}\sum_{i}^{B}(Q_\theta(\mathcal{O}_i,\mathcal{G}_i)-y_i)^2\,. \tag{7}$$

C. Feedback Augmented by ADG

In the existing work, e.g., [3], [7], [8], [10], the primitive feedback of self-supervised grasp learning is binary. If a grasp succeeds, grasp flag $g=1$, otherwise, $g=0$. However, it is too insufficient to evaluate the action quality of grasps, e.g., how the grasp destructs the environment. To facilitate a robot grasping like a human, we harness ADG to augment the primitive feedback of self-supervised grasp learning. In practice, we exploit a discrete ADG $\hat{\mathcal{A}}$ to encourage the grasp policy in collecting effective rewards.

$$\hat{\mathcal{A}}=\begin{cases}1 & if\ \ 0\le\mathcal{P}\le c_0\\ 1-c_i & if\ \ c_{i-1}<\mathcal{P}\le c_i\,, i\in[1,n]\subset\mathbb{N}.\\ 0 & if\ \ c_n<\mathcal{P}\le 1\end{cases} \tag{8}$$

$\hat{\mathcal{A}}$ is a discrete piecewise variant of $\mathcal{A}$. In Eq. (8), $\hat{\mathcal{A}}\in[0,1]$ is divided into n+2 segments. The relationship between $\hat{\mathcal{A}}$ and $\mathcal{P}$ as shown in Fig. S1 of an online supplementary file [35]. $\mathcal{C}=\{c_j\}_{j\in[0,n]}$ is used to adjust the sensitivity of ADG to DEG, called *destruction tolerance*. By experience, we set $c_j=\frac{j}{n+1}$. In general, the bigger c_j is, the more sensitive ADG to DEG is. Namely, it is more challenging to collect effective feedback during the learning process. In detail, ADG is combined with g to form augmented feedback,

$$\mathcal{R}(\hat{\mathcal{A}},g)=\begin{cases}e & if\ \ g=1,0\le\mathcal{A}\le 1-c_n\\ r+\hat{\mathcal{A}} & if\ \ g=1,1-c_n<\mathcal{A}\le 1\,,\\ 0 & if\ \ g=0\end{cases} \tag{9}$$

where c_n, r, and e are the maximum value of $\mathcal{C}$, a primary basic reward, and a secondary basic reward, respectively. We set $\mathcal{R}=0$ to suppress a failed grasp with $g=0$ during learning. For a successful grasp with $g=1$, a robot is encouraged to collect more effective feedback in the first two cases, i.e., $\mathcal{R}=e$ or $\mathcal{R}=r+\hat{\mathcal{A}}$. We set $e=0.5$, $r=1$ and r is more significant than e in preventing RA-Net from trapping into a local minimal.

D. Restorative Sampling Strategy

The existing strategies of grasp sample collection, e.g., in[3], [7]–[9], are not suitable to collect the samples with ADG. To obtain ADG, we develop a restorative sampling strategy or RSS for short given by **Algorithm A1** in [35].

Assume that the gripper is at its initial pose. First, a fixed mounted RGB-D camera captures the images of grasp environment, $I_i=(I_c,I_d)$. By projecting the RGB image I_c and depth image I_d along the vertical direction to yield in turn color and depth heightmap images, $I_{hc\,i}$ and $I_{hd\,i}$, or called an observation $\mathcal{O}_i=(I_{hc\,i},I_{hd\,i})$. ϵ-greedy policy adopted accepts $\mathcal{O}_i$ as inputs and outputs a grasp $\mathcal{G}_i=(T_i,\phi_i)$. Second, an instance of the restorative manipulation M_i is performed to obtain g_i and $\mathcal{O}_i^+=(I_{hc\,i}^+,I_{hd\,i}^+)$. Finally, we get $\mathcal{A}_i$, $\mathcal{R}_i$, and the i-th sample $(\mathcal{O}_i,\mathcal{G}_i,\mathcal{R}_i)$ by Eqs. (1), (8) and (9).

In Fig. 3, (1) a gripper moves first to $T_i^l=(x_i,y_i,z_i+l)$ and rotates ϕ_i around Z-axis, and then (2) moves to T_i along $\mathcal{T}_i$, where T_i^l is at height l right above $T_i=(x_i,y_i,z_i)$. Close the gripper and check whether it successfully grasps or not the object according to the distance between its two fingers. If it is a successful grasp, (3) the gripper moves backward to T_i^l along $\mathcal{T}_i^-$. If the object is not dropped during the return, $g_i=1$, and then (4) the robot places the object back to T_i along $\mathcal{T}_i$. After $\mathcal{G}_i$, the RGB-D camera captures $\mathcal{O}_i^+=(I_{hc\,i}^+,I_{hd\,i}^+)$, where $I_{hc\,i}^+$ and $I_{hd\,i}^+$ are the projection of $I_{c\ i}^+$ and $I_{d\ i}^+$ along the vertical direction, respectively. Finally, the robot (5) performs $\mathcal{G}_i$ again and (6) takes the object to the goal place. If the robot fails to grasp the object or loses it after picking up, $g=0$, and then the robot goes back to its home. The proccess executed by a real UR3 is illustrated in Fig. S2 of [35].

To train FAGL, $\epsilon-greedy$ policy is adopted to collect actions by exploitation and exploration according to Eq. (4) and a $random\ policy$ is used to sample actions under uniform distribution in robot workspace. The detailed process is given in **Algorithm A2** in [35]

Finally, the FAGL's inference process is to obtain an optimal grasp $\mathcal{G}^*$ given $Q_\theta^*(\mathcal{O},\mathcal{G})$. Note that the process of placing back a grasped object does not appear in inferences but in sample collection.

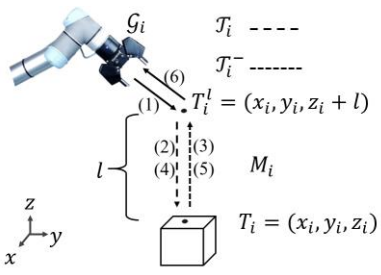

Fig. 3. The process of restorative sample collection.

E. RA-Net for Grasp Affordance Prediction

In general, grasp affordances [20], [33], [34] are dense pixel-wise probability maps of grasp success in image space. Nevertheless, each pixel of grasp affordances in FAGL indicate g and ADG. In other words, the closer the pixel value is to 1, the greater the successful grasp possibility and the higher ADG is, and vice versa.

Previous methods predict a rotated grasp affordance using a deep neural network, such as AIN in [8] and DenseNet in [7]. However, they suffer from a dilemma that the rotated affordance cannot represent a 2D position and an angle around Z-axis at the same time. They are obliged to rotate the input image and execute forward passes for several times to infer the optimal angle.

We propose a Refined Affordance Network (RA-Net) to directly infer a multi-channel grasp affordance $\mathcal{Q} = \{q_i\}_{i\in[1,C]\subset\mathbb{N}}$ for predicting the 2D position and the angle at the same time. $\mathcal{Q} \in \mathbb{R}^{H\times W\times C}$ is a three-dimensional affordance map consisting of C affordance planes $q_i \in \mathbb{R}^{H\times W}$ in sequence, where channels H, W are the height and width of $\mathcal{O}$. Similar to the previous method in [7], we set $H = W = 224$. Channel C denotes the number of rotation angles ϕ_i on plants q_i. We set C =18 and thereby the rotation increment is 360° /18=20° . By this way, RA-Net can avoid redundancy operation of rotating an input image and reduces the inference time. In addition, we also update the grasping action with the rotation angle opposite to $\mathcal{G}_i$ to improve the learning efficiency considering the symmetry of the parallel gripper.

RA-Net is composed of encoder, fusion, and decoder module, as shown in Fig. 2 (b). The encoder module accepts $\mathcal{O} = (I_{hc}, I_{hd})$ as its inputs and outputs a shallow color feature $\mathcal{V}_{sc}$ and a shallow depth feature $\mathcal{V}_{sd}$. In the encoder module, I_{hc} and I_{hd} are fed into a color encoder and a depth encoder, respectively. The fusion module takes $\mathcal{V}_{sc}$ and $\mathcal{V}_{sd}$ as its input and outputs a latent feature $\mathcal{V}_m$. $\mathcal{V}_m$ is the input of the decoder module that outputs $\mathcal{Q}$ with same size to I_{hc} and I_{hd}. Both the color and depth encoders are of the backbone, ResNet-50. The fusion module consists of two convolution blocks, each having two convolutional layers of a 3×3 kernel with 2048 or 64 channels and an activation function ReLU. The decoder module comprises three DeConvolution blocks and a bilinear upsample operation with an eight times scale. Every DeConvolution block with 32, 32 or 16 channels has two deconvolution layers of a 3×3 kernel and ReLU.

RA-Net is implemented with PyTorch 1.8. An ADAM optimizer is adopted to train RA-Net with 10^{-3} learning rate and a decay mechanism. RA-Net is trained by using the policy of prioritized experience replay.

F. Grasp Evaluation Metrics

Most previous studies only use grasp success rate (*GSR*) [7] to evaluate the performance of grasp learning.

$$GSR = \frac{K}{M}, \tag{10}$$

where M and K denote the times of all grasps and successful grasps, respectively. We also evaluate the average ADG (*AADG*) for grasps of many objects.

$$AADG = \frac{\sum^{M} \mathcal{A}_i}{M}, \tag{11}$$

where $\mathcal{A}_i$ denotes the antipodal degree of i-th grasp. A greater *AADG* indicates that a grasp causes less destruction to the environment. In addition, a mixed indicator F is defined as a weighted sum of *GSR* and *AADG* to achieve a better balance between them.

$$F = \alpha GSR + (1-\alpha)AADG, \alpha \in [0,1] \subset \mathbb{R}. \tag{12}$$

V. Experiments

A. Experimental Setup

Almost the existing DRL-based grasp methods only consider daily items of simple and basic shapes such as cubes and cones instead of actual metal workpieces. Generally, grasping metal workpieces requires more, e.g., on grasp position and orientation. In addition, metal workpieces may be of different kinds and pile up or occlude each other in a bin. It is still a big challenge for a robot to grasp them. Here, we try to grasp metal workpieces in different scenarios using our method presented.

An experiments system is set up with a UR3 robot containing a parallel gripper and an eye-to-hand mounted RealSense 415D camera, as shown in Fig. 4(a). Figure 4(b) illustrates 20 metal workpieces of different kinds in complicated shapes. The experiments are performed on a sever with Intel Xeon CPU E5-2620 v3 @ 2.4 Ghz and NVIDIA RTX 3090, installed Ubuntu 18.04. We set $n = 3$ in Eq. (8) to calculate ADG, and $M = 30$ and $\alpha = 0.5$ to calculate F.

B. Methods for Comparison and Training

We compare our method with the state-of-the-art self-supervised grasp learning methods. 1) The grasping-only version method in [7], called *Visual Grasp Learning (VGL)*, takes the success or failure of a grasp as feedback; 2) *Affordance Interpreter Network (AIN)* [8] generating antipodal grasps by training on antipodal samples; 3) *Affordance Space Perception Network (ASPN)* [33], an advanced affordance-based grasp detection methods; 4) *FC-GQ-CNN* [25], reaching antipodal and collision-free grasp by training on a large-scale comprehensive dataset.

Similar to the training process in VGL [11], our FAGL and VGL are trained 2500 times in Coppeliasim [41] to grasp 9 different 3D toy blocks, and then trained 500 times of grasping metal workpieces in the real environment. The shapes and colors of 3D toy blocks in the simulation are randomly chosen during training. We collect 500 grasp samples of 20 kinds metal workpieces to fine-tune FC-GQ-CNN, AIN, and ASPN for fair comparison. UR3 repeats to grasp workpieces until its workspace is emptied or it fails to grasp for over ten times. All workpieces are randomly placed into UR3's workspace manually in advance.

(a) (b) (c)

Fig. 4. Experimental setup. (a) UR3 grasp system, (b) 20 kinds of metal workpieces, and (c) six kinds of unseen objects.

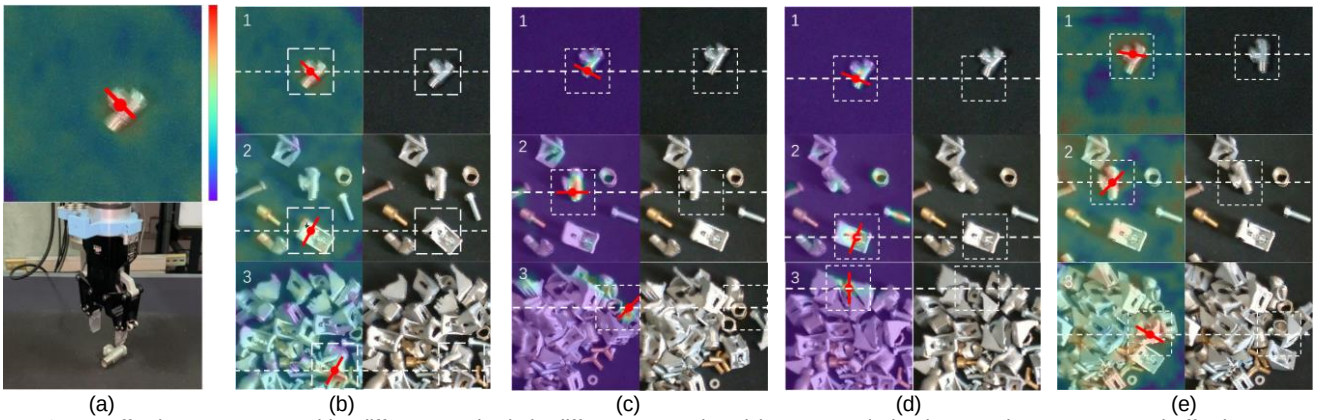

(a) (b) (c) (d) (e)

Fig. 5 Grasp affordances generated by different methods in different scenarios. (a) an example is given to show a generated affordance map with optimal grasp position and direction denoted by a red line and a red point, and the corresponding actual grasp. (b)-(e) show the grasp affordance maps (in each first column) and the color heightmaps after restorative manipulation (in each second column) using FAGL, AIN, ASPN, and VGL in different scenarios with a single object (1), scattered objects (2), and cluttered objects (3), respectively.

C. Grasping in Various Scenarios

We consider three scenarios with a single object, scattered objects, and cluttered objects. In the second scenario, there is no occlusion between the workpieces. In the third scenario, the workpieces are severely piled up and occluded each other. Therefore, a poor grasp may seriously destroy the layout of workpieces. Next, we evaluate our method and its competitors in such scenarios.

Figure 5 show grasp affordances generated by FAGL and AIN, ASPN, and VGL in different scenarios. Figure 5 shows the generated affordance maps with the same resolution as the corresponding color heightmaps, and the pixel closer to red, the higher the grasp success rate. The white dash lines and boxes are exploited to indicate the original positions of the objects before grasps. FC-GQ-CNN is absent because it does not rely on grasp affordances. All methods can successfully grasp objects, but their ADG are quite different. As illustrated in the color heightmap after a restorative manipulation in Fig. 5(b), FAGL can successfully grasp the object marked by a red point with slightly destructing or even without destructing its surroundings in the scenarios with a single object, scattered objects, and cluttered objects. It demonstrates the grasps using FAGL have a high ADG, i.e., the grasp point on the object is nearly collinear to the normal of the contact points. FAGL avoids the perturbation to the environment caused by the collision between the gripper and objects. As shown in the first and second rows in Fig. 5(c), AIN generates antipodal grasp or near antipodal grasp in the scenarios with single object and scattered objects. However, it fails to generate antipodal grasps in the cluttered scene, as shown in the third row of Fig. 5(c). ASPN and VGL successfully grasp the object but destructs its surroundings in the object scenarios with a single object, scattered objects, and cluttered objects, as shown in Fig. 5(d) and (e). It suggests that ASPN and VGL cannot provide grasps with a high ADG because they do not take grasp quality into account.

Next, we compare FAGL with AIN, ASPN, VGL in terms of *GSR* and *AADG* considering different grasp scenarios. Table I shows all methods achieve high *GSR* in single-object scenarios. Our method and FC-GQ-CNN achieve a very close and highest *AADG*. It indicates that they are most likely to avoid unexpected movements of a single object during grasp, such as unexpected rotation of the object, in a simple scenario. But VGL and ASPN are very likely to incur unexpected movements of an object during grasp. This problem is more apparent when the robot attempts to grasp elongated objects, e.g., pencils, ticks, and shafts.

Unexpected movements of an object being grasped may cause changes in a grasp scene.

Our FAGL achieves *GSR*=0.87 in scattered-object cases. It is comparable to FC-GQ-CNN and AIN. On the other hand, our method exceeds all its peers in *AADG*. It indicates that our method is more suitable for grasping scattered objects and results in higher *ADG*. Nevertheless, the *AADG* of FC-GQ-CNN and AIN drop dramatically in the same scenarios since antipodal grasps have not been considered in the training stage.

In cluttered scenarios, our method achieves the highest *GSR*, *AADG*, and *F*, as shown in Table I. It means that our method can grasp cluttered objects with a higher *ADG* and *GSR*. The reason is in that the augmented feedback can guide a robot to adjust *ADG* in a fine-grained manner in response to various scenarios. FAGL outperforms significantly over AIN that is designed to generate antipodal grasps in a variety of circumstances [8]. However, AIN brings greater *DEG* in most cluttered cases and cannot well adjust ADG as FAGL does when confronted with various scenarios.

Moreover, we compare our FAGL with ASPN, VGL, AIN, and FC-GQ-CNN in inference time. Our FAGL, ASPN, VGL, AIN, and FC-GQ-CNN take 14ms, 6ms, 51ms, 2.5s, and 0.625s, respectively. It indicates that our FAGL is faster than AIN, VGL, and FC-GQ-CNN due to predict a multi-channel affordance without rotation operation. On the other hand, our FAGL is slightly slower than ASPN since FAGL needs to dispose additional depth information.

D. Grasping Unseen Objects

Several experiments are conducted over the six kinds of unseen metal workpieces to test the generalizability of FAGL, as shown in Fig. 4(c). Its evaluation protocols and metrics are identical to those used above. The experimental results are presented in Table II. Our method achieves a competitive *GSR* and the highest *AADG* when grasping novel objects in different scenarios, especially in

TABLE I
COMPARISON OF METHODS IN DIFFERENT SCENARIOS

Scenarios	Single object			Scattered objects			Cluttered objects		
Metrics / Methods	*GSR*	*AADG*	*F*	*GSR*	*AADG*	*F*	*GSR*	*AADG*	*F*
VGL	0.89	0.48	0.69	0.85	0.21	0.53	0.72	0.09	0.41
FC-GQ-CNN	**0.95**	0.88	**0.92**	**0.88**	0.64	0.76	0.81	0.37	0.59
AIN	0.91	0.82	0.87	0.86	0.48	0.67	0.79	0.21	0.50
ASPN	0.94	0.66	0.80	0.85	0.37	0.61	0.77	0.15	0.46
FAGL	0.93	**0.89**	0.91	0.87	**0.66**	**0.77**	**0.82**	**0.56**	**0.69**

TABLE II
COMPARISON OF METHODS IN GRASPING UNSEEN OBJECTS

Scenarios	Single object			Scattered objects			Cluttered objects		
Metrics / Methods	*GSR*	*AADG*	*F*	*GSR*	*AADG*	*F*	*GSR*	*AADG*	*F*
VGL	0.90	0.38	0.64	0.78	0.19	0.49	0.69	0.09	0.39
FC-GQ-CNN	**0.94**	0.78	0.86	**0.83**	0.54	0.69	0.75	0.39	0.57
AIN	0.93	0.78	0.86	0.78	0.51	0.65	0.74	0.17	0.46
ASPN	0.91	0.61	0.76	0.81	0.32	0.57	0.69	0.13	0.41
FAGL	0.93	**0.81**	**0.87**	0.82	**0.62**	**0.72**	**0.78**	**0.48**	**0.63**

TABLE III
PERFORMANCE COMPARISON OF FAGL UNDER DIFFERENT DESTRUCTION TOLERANCE

Scenarios	Single object			Scattered objects			Cluttered objects		
Metrics / Destruction Tolerance	*GSR*	*AADG*	*F*	*GSR*	*AADG*	*F*	*GSR*	*AADG*	*F*
$\mathcal{C}_t$	0.93	0.66	0.80	0.88	0.35	0.62	0.84	0.21	0.53
$\mathcal{C}_r$	0.91	0.54	0.73	0.71	0.44	0.58	0.75	0.18	0.47

cluttered ones. It implies that our method has better generalizability than its peers. Such generalizability enables not only the successful grasping of novel objects, as done in [2], [5], but also fine-grained antipodal grasps in various environments.

E. Grasping with Different Destruction Tolerance

$\mathcal{C}$ is multiplied by a scaling factor δ to adjust the sensitivity of *ADG* to *DEG*. Specifically, we can tighten and relax $\mathcal{C}$ by multiplying the coefficients $\delta_t = 1/2$ and $\delta_r = 2$, respectively. Accordingly, we obtain $\mathcal{C}_t = \{\delta_t c_j\}$ and $\mathcal{C}_r = \{\delta_r c_j\}, j \in [0, n]$. Note that, even given the same *DEG*, *AADG* are distinct if different $\mathcal{C}$ are used. Thus, for a fair comparison, we use $\mathcal{C}$ to obtain *AADG* for evaluating the impact of adjusting $\mathcal{C}$ on the performance of FAGL.

The effects of using $\mathcal{C}_t$, and $\mathcal{C}_r$ are summarized in Table III. $\mathcal{C}$, $\mathcal{C}_t$, and $\mathcal{C}_r$ achieve similar *GSR* in grasping a single object, scattered objects, and cluttered objects. What stands out in Table III is that grasping with $\mathcal{C}_t$ can achieve a higher *GSR* in cluttered environments, and grasping under $\mathcal{C}_t$ and $\mathcal{C}_r$ results in a lower *AADG* than grasping under $\mathcal{C}$ does in all environments. It is most likely because the destruction tolerance affects the generation of effective feedback to the grasp policy. In detail, excessively pursuing low *DEG* may impede the obtaining of the primary reward r and increases the difficulty of collecting grasp samples with

a high *ADG*. On the other hand, usually, $\mathcal{C}_r$ can ease Q_θ to obtain grasp feedback with a higher *GSR* but lower *AADG*. However, too high destruction tolerance may lead to deceptive feedback that misinterprets a disastrous *DEG* for a superior *ADG*. In a word, by properly adjusting $\mathcal{C}$, it is possible to effectively direct a grasp policy by balancing *GSR* and *AADG*.

VI. Conclusion

This work proposes a self-supervised learning method, FAGL, for fine-grained antipodal grasp. FAGL consists of augmented feedback, RSS, and RA-Net. First, antipodal degree of a grasp (ADG) is defined to evaluate grasp quality in a fine-grained manner by measuring destructive effect of a grasp in image space. By taking ADG into account, the learning feedback is augmented to a fine-grained extent. We use RSS to collect the samples of fine-grained antipodal grasps. RA-Net is developed to generate multi-channel grasp affordances for FAGL to decide an optimal grasp. Finally, FAGL is compared with the existing methods, AIN, VGL, ASPN, and FC-GQ-CNN, in grasping metal workpieces. The extensive experiments show that our FAGL achieves 82% grasp success rate and 0.56 average ADG in cluttered environments and outperforms its four peers in most environments. Our ongoing work is to merge the end-effector forces into the feedback of grasp leaning to realize safe grasp in a self-supervised manner.

References

[1] J. Mahler *et al.*, "Learning ambidextrous robot grasping policies," *Sci. Robot.*, vol. 4, no. 26, 2019.
[2] J. Bohg, A. Morales, T. Asfour, and D. K. Member, "Data-Driven Grasp Synthesis - A Survey," *Trans. Robot.*, vol. 30, no. 2, pp. 289–309, 2014.
[3] L. Pinto and A. Gupta, "Supersizing self-supervision: Learning to grasp from 50K tries and 700 robot hours," *Proc. - IEEE Int. Conf. Robot. Autom.*, vol. 2016-June, pp. 3406–3413, 2016.
[4] A. Bicchi and V. Kumar, "Robotic grasping and contact: A review," *Proceedings-IEEE Int. Conf. Robot. Autom.*, vol. 1, pp. 348–353, 2000.
[5] S. Y. Shin and C. Kim, "Human-Like Motion Generation and Control for Humanoid ' s Dual Arm Object Manipulation," *IEEE Trans. Ind. Electron.*, vol. 62, no. 4, pp. 2265–2276, 2015.
[6] W. Fang *et al.*, "Visual-Guided Robotic Object Grasping Using Dual Neural Network Controllers," *IEEE Trans. Ind. Informatics*, vol. 17, no. 3, pp. 2282–2291, 2021.
[7] A. Zeng, S. Song, S. Welker, J. Lee, A. Rodriguez, and T. Funkhouser, "Learning Synergies between Pushing and Grasping with Self-Supervised Deep Reinforcement Learning," *IEEE Int. Conf. Intell. Robot. Syst.*, pp. 4238–4245, 2018.
[8] J. Cai, H. Cheng, Z. Zhang, and J. Su, "MetaGrasp: Data efficient grasping by affordance interpreter network," *Proc. - IEEE Int. Conf. Robot. Autom.*, vol. 2019-May, pp. 4960–4966, 2019.
[9] Y. Deng *et al.*, "Deep Reinforcement Learning for Robotic Pushing and Picking in Cluttered Environment," in *IEEE/RSJ International Conference on Intelligent Robots and Systems (IROS)*, 2019, pp. 619–626.
[10] S. Levine, P. Pastor, A. Krizhevsky, J. Ibarz, and D. Quillen, "Learning hand-eye coordination for robotic grasping with deep learning and large-scale data collection," *Int. J. Rob. Res.*, vol. 37, no. 4–5, pp. 421–436, 2018.
[11] A. Bicchi, "On the Closure Properties of Robotic Grasping," *Int. J. Rob. Res.*, vol. 14, no. 4, pp. 319–334, 1995.
[12] A. Pas and R. Platt, "Using Geometry to Detect Grasp Poses in 3D Point Clouds," in *12th International Symposium on Robotics Research (ISRR)*, 2015, pp. 307–324.
[13] M. A. Roa and R. Suárez, "Grasp quality measures: review and performance," *Auton. Robots*, vol. 38, no. 1, pp. 65–88, 2015.
[14] Z. He, C. Wu, S. Zhang, and X. Zhao, "Moment-Based 2.5-D Visual Servoing for Textureless Planar Part Grasping," *IEEE Trans. Ind. Electron.*, vol. 66, no. 10, pp. 7821–7830, 2019.
[15] I. Lenz, H. Lee, and A. Saxena, "Deep learning for detecting robotic grasps," *Int. J. Rob. Res.*, vol. 34, no. 4–5, pp. 705–724, 2015.
[16] K. Dmitry *et al.*, "Scalable Deep Reinforcement Learning for Vision-Based Robotic Manipulation," in *Conference on Robot Learning*, 2018, pp. 651–673.
[17] J. Wang, Y. Liu, and B. Li, "Reinforcement learning with perturbed rewards," *34th AAAI Conf. Artif. Intell.*, pp. 6202–6209, 2020.
[18] C. Colas, P. Fournier, O. Sigaud, M. Chetouani, and P.-Y. Oudeyer, "CURIOUS: Intrinsically Motivated Modular Multi-Goal Reinforcement Learning," 2019.
[19] T. Tan, F. Bao, Y. Deng, A. Jin, Q. Dai, and J. Wang, "Cooperative deep reinforcement learning for large-scale traffic grid signal control," *IEEE Trans. Cybern.*, vol. 50, no. 6, pp. 2687–2700, 2020.
[20] H. Liu, Y. Deng, D. Guo, B. Fang, F. Sun, and W. Yang, "An Interactive Perception Method for Warehouse Automation in Smart Cities," *IEEE Trans. Ind. Informatics*, vol. 17, no. 2, pp. 830–838, 2021.
[21] L. Berscheid, P. Meisner, and T. Kroger, "Self-Supervised Learning for Precise Pick-and-Place without Object Model," *IEEE Robot. Autom. Lett.*, vol. 5, no. 3, pp. 4828–4835, 2020.
[22] T. Tan, R. Alqasemi, R. Dubey, and S. Sarkar, "Formulation and Validation of an Intuitive Quality Measure for Antipodal Grasp Pose Evaluation," *IEEE Robot. Autom. Lett.*, vol. 6, no. 4, pp. 6907–6914, 2021.
[23] I. Chen and J. W. Burdick, "Finding antipodal point grasps on irregularly shaped objects," *IEEE Trans. Robot. Autom.*, vol. 9, no. 4, pp. 507–512, 1993.
[24] J. Mahler, J. Liang, S. Niyaz, M. Laskey, R. Doan, and X. Liu, "Dex-Net 2 . 0 : Deep Learning to Plan Robust Grasps with Synthetic Point Clouds and Analytic Grasp Metrics," 2017.
[25] V. Satish, J. Mahler, and K. Goldberg, "On-policy dataset synthesis for learning robot grasping policies using fully convolutional deep networks," *IEEE Robot. Autom. Lett.*, vol. 4, no. 2, pp. 1357–1364, 2019.
[26] Y. Qin, R. Chen, H. Zhu, M. Song, J. Xu, and H. Su, "S4G:Amodal Single-view Single-Shot SE(3) Grasp Detection in Cluttered Scenes," in *Conference on robot learning*, 2020, pp. 53–65.
[27] H. Liang *et al.*, "PointNetGPD : Detecting Grasp Configurations from Point Sets," in *IEEE International Conference on Robotics and Automation (ICRA)*, 2019, pp. 3629–3635.
[28] A. ten Pas, M. Gualtieri, K. Saenko, and R. Platt, "Grasp Pose Detection in Point Clouds," *Int. J. Rob. Res.*, vol. 36, no. 13–14, pp. 1455–1473, 2018.
[29] V. Mnih *et al.*, "Human-level control through deep reinforcement learning," *Nature*, vol. 518, no. 7540, pp. 529–533, 2015.
[30] H. Van Hasselt, A. Guez, and D. Silver, "Deep Reinforcement Learning with Double Q-learning," in *30th AAAI Conference on Artificial Intelligence*, 2016, pp. 2094–2100.
[31] S. Iqbal *et al.*, "Toward Sim-to-Real Directional Semantic Grasping," in *Proceedings - IEEE International Conference on Robotics and Automation*, 2020, pp. 7247–7253.
[32] S. Joshi, S. Kumra, and F. Sahin, "Robotic Grasping using Deep Reinforcement Learning," in *IEEE International Conference on Automation Science and Engineering*, 2020, vol. 2020-Augus, pp. 1461–1466.

[33] H. Wu, Z. Zhang, H. Cheng, K. Yang, J. Liu, and Z. Guo, "Learning Affordance Space in Physical World for Vision-based Robotic Object Manipulation," *Proc. - IEEE Int. Conf. Robot. Autom.*, pp. 4652–4658, 2020.
[34] D. Morrison, P. Corke, and J. Leitner, "Learning robust, real-time, reactive robotic grasping," *Int. J. Rob. Res.*, vol. 39, no. 2–3, pp. 183–201, 2020.
[35] Supplementary File, 2022. [Online]. Available: https://github.com/houyanxu/FAGL/blob/main/R1_Supplementary_File_Final.pdf.

Yanxu Hou received the B.S. degree from the Anhui Jianzhu University, Hefei, China, in 2015, and the M.S. degree from the Hefei University of Technology, Hefei, China, in 2018. He is currently pursuing the Ph.D. degree at Southeast University, Nanjing, China.

His research interests include reinforcement learning and robotic grasp.

Jun Li (Senior Member, IEEE) received Ph.D. degree in control theory and control engineering from Southeast University (SEU), Nanjing, China, in 2007.

In 2014, he was a Visiting Scholar with the New Jersey Institute of Technology, Newark, NJ, USA. His current research interests include logistics and construction robotics, machine vision, machine learning, and operations research.

Professor Li is a Fellow of the Institution of Engineering and Technology (IET) and serves as an Associate Editor for IEEE TRANSACTIONS ON INTELLIGENT TRANSPORTATION SYSTEMS.

I-Ming Chen (Fellow, IEEE) received B.S. degree from National Taiwan University, Taipei, Taiwan, in 1986, and M.S. and Ph.D. degrees from the California Institute of Technology, Pasadena, in 1989 and 1994, respectively. He has been with the School of Mechanical and Aerospace Engineering of Nanyang Technological University (NTU) in Singapore since 1995. He was a Japan Society for the Promotion of Science (JSPS) Visiting Scholar at Kyoto University, Kyoto, Japan in 1999, a Visiting Scholar in the Department of Mechanical Engineering, Massachusetts Institute of Technology (MIT), in 2004. He was Director of Robotics Research Centre (2013 to 2017), and Director of Intelligent Systems (2006 to 2015) in NTU. His research interests are in construction and logistics robots, wearable devices, human-robot interaction and industrial automation. Professor Chen was General Chairman of 2017 *IEEE International Conference on Robotics and Automation* (ICRA 2017) in Singapore, Fellow of ASME, and Fellow of Academy of Engineering, Singapore. He is Editor-in-chief of IEEE/ASME TRANSACTIONS ON MECHATRONICS from 2020 to 2022.